The Impact of AIRS Atmospheric Temperature and Moisture Profiles on Hurricane Forecasts: Ike (2008) and Irene (2011)

ZHENG Jing*[1,2], Jun LI[1], Timothy J. SCHMIT[3], Jinlong LI[1], and Zhiquan LIU[4]

[1]*Cooperative Institute for Meteorological Satellite Studies, University of Wisconsin-Madison, Wisconsin* 53706, *USA*
[2]*National Satellite Meteorological Center, China Meteorological Administration, Beijing* 100081
[3]*Advanced Satellite Products Branch, Center for Satellite Applications and Research, NESDIS/NOAA, Madison, WI* 53706, *USA*
[4]*National Center for Atmospheric Research, Boulder, Colorado* 80305, *USA*

(Received 9 August 2013; revised 10 April 2014; accepted 27 June 2014)

ABSTRACT

Atmospheric InfraRed Sounder (AIRS) measurements are a valuable supplement to current observational data, especially over the oceans where conventional data are sparse. In this study, two types of AIRS-retrieved temperature and moisture profiles, the AIRS Science Team product (SciSup) and the single field-of-view (SFOV) research product, were evaluated with European Centre for Medium-Range Weather Forecasts (ECMWF) analysis data over the Atlantic Ocean during Hurricane Ike (2008) and Hurricane Irene (2011). The evaluation results showed that both types of AIRS profiles agreed well with the ECMWF analysis, especially between 200 hPa and 700 hPa. The average standard deviation of both temperature profiles was approximately 1 K under 200 hPa, where the mean AIRS temperature profile from the AIRS SciSup retrievals was slightly colder than that from the AIRS SFOV retrievals. The mean SciSup moisture profile was slightly drier than that from the SFOV in the mid troposphere. A series of data assimilation and forecast experiments was then conducted with the Advanced Research version of the Weather Research and Forecasting (WRF) model and its three-dimensional variational (3DVAR) data assimilation system for hurricanes Ike and Irene. The results showed an improvement in the hurricane track due to the assimilation of AIRS clear-sky temperature profiles in the hurricane environment. In terms of total precipitable water and rainfall forecasts, the hurricane moisture environment was found to be affected by the AIRS sounding assimilation. Meanwhile, improving hurricane intensity forecasts through assimilating AIRS profiles remains a challenge for further study.

Key words: AIRS, data assimilation, temperature profile, moisture profile, hurricane forecast, WRF, 3DVAR

Citation: Zheng, J., J. Li, T. J. Schmit, J. L. Li, and Z. Q. Liu, 2015: The impact of AIRS atmospheric temperature and moisture profiles on hurricane forecasts: Ike and Irene. *Adv. Atmos. Sci.*, **32**(3), 319–335, doi: 10.1007/s00376-014-3162-z.

1. Introduction

The increase in satellite remote sensing data has led to significant advances in improving weather forecasts, particularly for severe weather such as tropical cyclones (TCs). Two of the most important observations are the atmospheric temperature and moisture observations in the TC's environment. Their assimilation in numerical weather prediction (NWP) models helps improve the TC's prediction, and thus provides forecasts of higher accuracy and greater reliability for decision making and public response (e.g., Leidner et al., 2003; Zhang et al., 2007; Chen et al., 2008; Pu et al., 2009; Reale et al., 2009; Liu and Li, 2010).

Improvements in the measurement capabilities of satellite instruments, such as the Atmospheric Infrared Sounder (AIRS), the Infrared Atmospheric Sounding Interferometer (IASI), the Cross-track Infrared Sounder (CrIS), the Advanced Microwave Sounding Unit (AMSU), and the Advanced Technology Microwave Sounder (ATMS), have played a critical role in better observations of the distribution of atmospheric temperature and moisture. Among these instruments, the infrared sounders such as AIRS, IASI and CrIS can measure the vertical distribution of atmospheric temperature and moisture in clear-sky and some cloudy conditions with high vertical and spatial resolutions, while the microwave instruments such as AMSU and ATMS can measure temperature and moisture in both clear-sky and cloudy-sky conditions with coarser spatial resolution.

To assimilate remotely sensed temperature and moisture information into an NWP model, either one of two approaches is followed: assimilating the radiances, or assimilating the retrievals. Currently, most leading NWP centers assimilate the satellite radiances directly into the data assimilation system (DAS) (e.g., Derber and Wu, 1998; Lorenc et al., 2000). This method requires the use of a radiative trans-

* Corresponding author: ZHENG Jing
Email: zhengjing@cma.gov.cn

fer model as the forward operator (i.e., observation operator) that maps model states into the measurement space. Thus, the assimilation process is computationally expensive, especially for hyperspectral instruments with thousands of channels, such as AIRS and IASI. Assimilating the retrievals is relatively easier and computationally efficient in the DAS. The retrieval data are usually expressed in the form of geophysical fields, such as temperature and moisture profiles, so that the comparison between model states and observations can be done via a simple spatial interpolation. Its main concern is that the errors in the retrievals can be correlated with the state, and hence with errors in the short-range forecast used as a constraint for the ill-posed problem of converting radiances into retrievals (Migliorini et al., 2008; Migliorini, 2012). Despite the pros and cons of each approach, there has been a renewed interest in assimilating AIRS retrievals in recent years with continued efforts to validate (e.g., Divakarla et al., 2006; Tobin et al., 2006) and improve retrieval algorithms (e.g., Susskind, 2007; Li and Li, 2008; Kwon et al., 2012; Smith et al., 2012; Susskind et al., 2012). Recent studies have shown that assimilating AIRS retrievals can have a positive impact on improving weather forecast skill (e.g., Zavodsky et al., 2007; Reale et al., 2008), contributing especially to hurricane forecasts (e.g., Li and Liu, 2009; Pu and Zhang, 2010; Miyoshi and Kunii, 2012). However, these studies validated and assimilated only one type of AIRS sounding product—either the AIRS Science Team product or the single field-of-view (SFOV) research product from the Cooperative Institute for Meteorological Satellite Studies (CIMSS) (Li and Huang, 1999; Li et al., 2000; Kwon et al., 2012). Not enough attention has been given to comparing different retrievals and their impacts on TC forecasts. It is not clear how well different types of retrievals represent the "truth" state in the hurricane environment, and what their impact on TC forecasts is if they are assimilated into a regional NWP model. By applying the same algorithm, the AIRS Science Team produces standard products (AIRX2RET) with 28 standard vertical pressure levels for temperature profiles and 14 pressure layers for moisture profiles, along with support products (AIRX2SUP; SciSup hereafter) with 100 pressure levels for temperature and moisture profiles. Due to their high vertical resolution, the SciSup products were chosen in this study to match with the SFOV products. Therefore, the objective of this study was to evaluate and assimilate two types of AIRS retrievals from AIRS Science Team SciSup and CIMSS research SFOV products in the hurricane environment and compare their common and different impacts on TC forecasts for better use of AIRS sounding information in regional NWP models.

In section 2, two types of AIRS sounding retrievals are compared and evaluated against the European Centre for Medium-Range Weather Forecasting (ECMWF) high spatial resolution global analysis. In section 3, results are reported from assimilating these AIRS retrievals into the Advanced Research version of the Weather Research and Forecasting (WRF) model with a three-dimensional variational (3DVAR) data assimilation system for two hurricane cases over the Atlantic Ocean via a series of cycling assimilation and forecast experiments. Their impacts on the hurricane track and intensity forecasts are shown in section 4. Finally, some brief concluding remarks are provided in section 5.

2. AIRS sounding retrievals and evaluation

2.1. *AIRS Instrument*

AIRS is carried on the National Aeronautics and Space Administration's (NASA's) Earth Observing System (EOS) Aqua satellite, which was launched in May 2002 and flies in a near-polar low-Earth orbit at an altitude of 705 km. As the first space-based hyperspectral infrared (IR) sounder, it covers the 3.7–15.4 μm spectral range, with 2378 spectral channels, and hence provides atmospheric temperature and moisture profile information with high vertical resolution. The horizontal resolution of AIRS is approximately 13.5 km at nadir and the swath width is 1650 km (Aumann et al., 2003; Parkinson, 2003; Chahine et al., 2006). In the past decade, AIRS has been highlighted for measuring atmospheric temperature and moisture profiles (e.g., Tobin et al., 2006; Susskind et al., 2012) and improving weather prediction by regional and global NWP models through assimilating its radiances (e.g., Le Marshall et al., 2006; McCarty et al., 2009) and retrievals (e.g., Atlas, 2005; Jedlovec et al., 2006; Liu and Li, 2010).

2.2. *CIMSS SFOV sounding retrievals*

The CIMSS hyperspectral IR Sounder Retrieval (CHISR) algorithm has been developed to simultaneously retrieve atmospheric temperature and moisture profiles from advanced IR sounder radiance measurements in clear-sky and some cloudy conditions on a SFOV basis (Li and Huang, 1999; Li et al., 2000; Zhou et al., 2007; Weisz et al., 2007). Its first guess comes from a regression method based on a global training dataset that consists of 15 704 atmospheric profiles and their corresponding simulated AIRS radiances (Weisz et al., 2007, 2013). The Moderate Resolution Imaging Spectrometer (MODIS) level 2 cloud mask data were used to identify the AIRS clear pixels (Li et al., 2004). Radiance measurements from 1450 good AIRS channels were used in the 1DVAR based physical iterative retrieval method for atmospheric temperature, moisture and ozone simultaneously with the Stand-alone AIRS Radiative Transfer Algorithm (SARTA) used as the forward model (Strow et al., 2003, 2006). The SFOV retrieval algorithm takes the total precipitable water (TPW) classification in the background error covariance matrix, and adopts a CO_2 adjustment in the retrieval algorithm. It also contains six quality control flags in the output to check non-converged or bad retrievals, large residuals, high terrain and desert areas (Kwon et al., 2012). With a horizontal resolution of approximately 13.5 km at nadir and 101 pressure levels vertically ranging from 1100 hPa at the bottom to 0.005 hPa at the top, these data can provide the atmospheric vertical temperature and moisture structures in the hurricane environment.

2.3. *AIRS Science Team sounding product*

A single sounding from the AIRS Science Team products was produced using all nine AIRS FOVs falling within a single AMSU footprint. Based on the AMSU/AIRS cloud-clearing algorithm, the retrieval process was separated into sequential steps to retrieve surface parameters, atmospheric temperature, moisture and other constituent profiles, and cloud properties. Each step used its own subset of channels. Geophysical parameters and observed AIRS radiances were used to generate an alternative initial state used for initial cloud clearing, but the cloudy regression made use of both AIRS and AMSU observations or AIRS observations only (Susskind et al., 2003, 2006, 2011). The SARTA accounting for non-local thermodynamic equilibrium (non-LTE) was used as the forward model (Strow et al., 2006). The final retrievals used were AIRX2SUP (i.e., SciSup) from the AIRS Level-2 Version 5 support products (Susskind, 2007; Won, 2008; Susskind et al., 2011) with a horizontal resolution of 45 km at nadir and 100 vertical pressure levels (between 1100 and 0.016 hPa), which match the vertical levels of the CIMSS SFOV products, except at the very top level (0.005 hPa). The SciSup's mixing ratio was calculated from its column vapor density in order to obtain its specific humidity. According to the data quality flags, the "PBest" flag indicates that the temperature profile from the top of the atmosphere (TOA) to

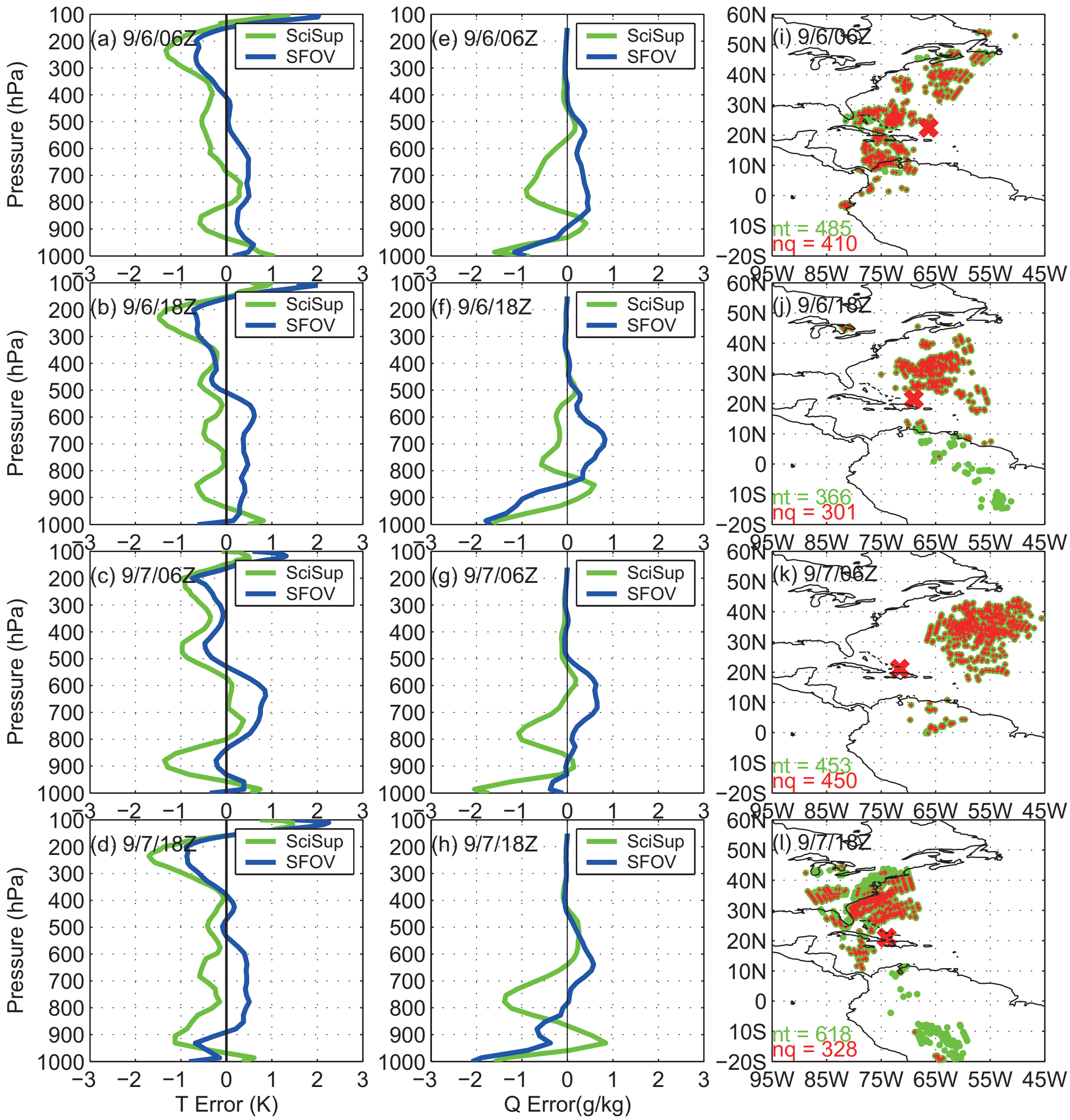

Fig. 1. Evaluation of AIRS retrievals against ECMWF reference data for Hurricane Ike (2008). The n_t (green) and n_q (red) stand for the number of profiles for temperature and moisture, respectively. Positive (negative) values in (a–h) indicate a warm (cold) or moist (dry) bias. The red cross shows the hurricane location.

that particular pressure level is of the best quality; while the "Qual_H_2O = 0" flag indicates the entire moisture profile is of the best quality. To control the quality of the retrievals, both criteria were applied.

2.4. *Retrieval evaluation*

Because of the lack of radiosonde observations over the ocean, the ECMWF analysis with $0.25° \times 0.25°$ resolution is used as a reference. Considering the rapid atmospheric temporal and spatial variation, only those AIRS data whose observation time was within 1 hour of the ECMWF analysis time were collocated. Meanwhile, the ECMWF grids were matched with the closest AIRS pixels, and 91-level ECMWF profiles were interpolated to AIRS pressure levels, similar to Kwon et al. (2012). The evaluation results showed that the vertical structures of the atmospheric temperature and moisture profiles from both types agreed well with the ECMWF analysis from the bottom to the tropopause. Figure 1 shows that the vertical mean temperature deviations for both types of AIRS retrievals were approximately 1 K under 200 hPa during Hurricane Ike from 0600 UTC 06 September to 1800 UTC 07 September 2008. The standard deviations (STD) for both types of AIRS temperature profiles were approximately 1 K between 200 hPa and 700 hPa. The mean SFOV temperature profile was slightly warmer than that of SciSup (Figs. 1a–d). Their mean moisture profiles showed both deviations were within 1 g kg^{-1} at 700 hPa. SciSup was slightly drier than SFOV between 500 hPa and 850 hPa (Figs. 1e–h). The evaluations during Hurricane Irene from 1800 UTC 23 August to 1800 UTC 24 August 2011 produced similar results. Correspondingly, the temperature and moisture profiles of best quality between 200 hPa and 700 hPa were selected

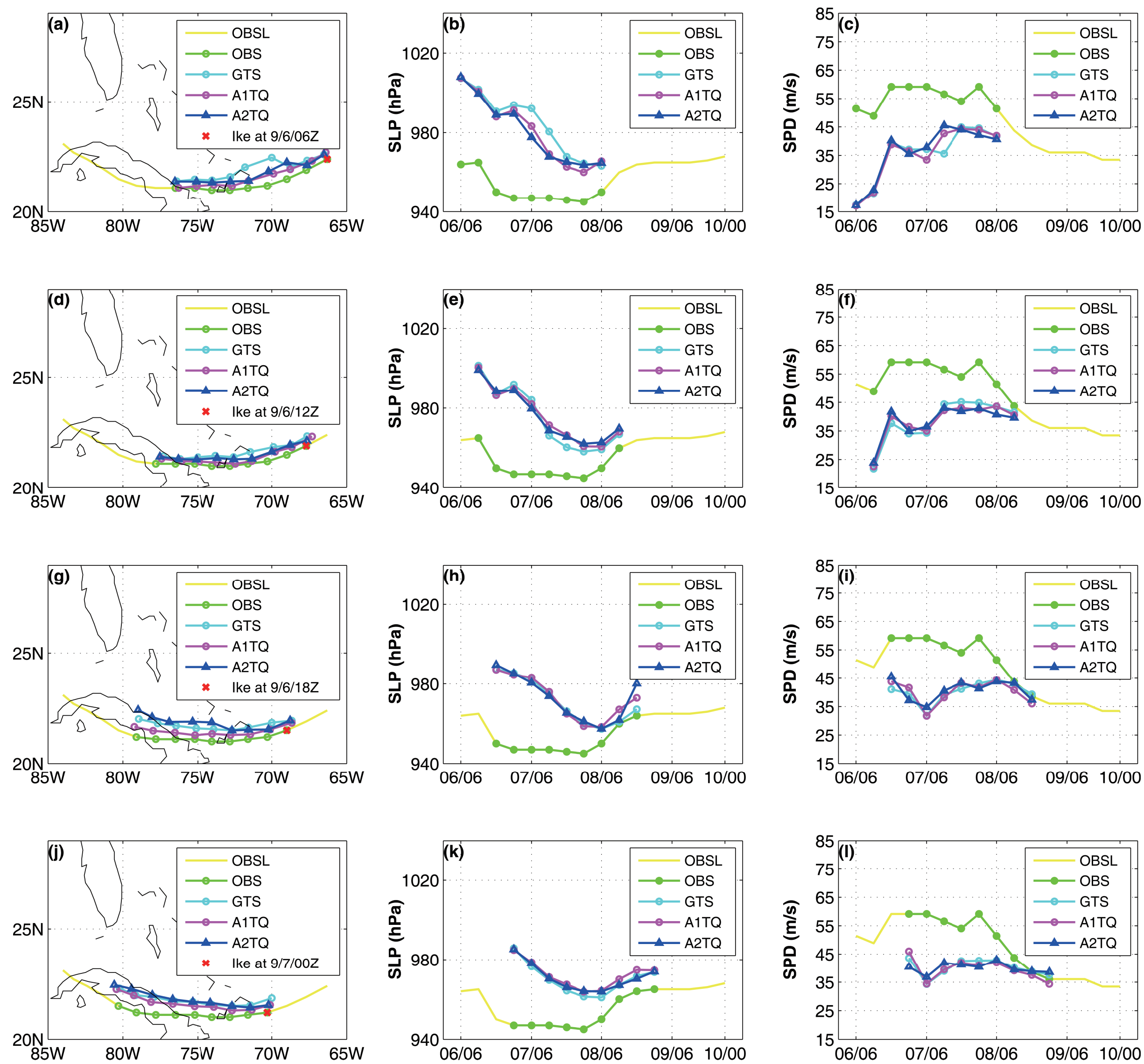

Fig. 2. The 48 h forecast results for Hurricane Ike (2008). The (a–d) HT, (e–h) SLP and (i–l) SPD from the GTS, A1TQ and A2TQ experiments are shown against the best hurricane record (OBS) during 6–10 September 2008. OBSL is the best record during the period from 0600 UTC 06 September to 1800 UTC 09 September 2008.

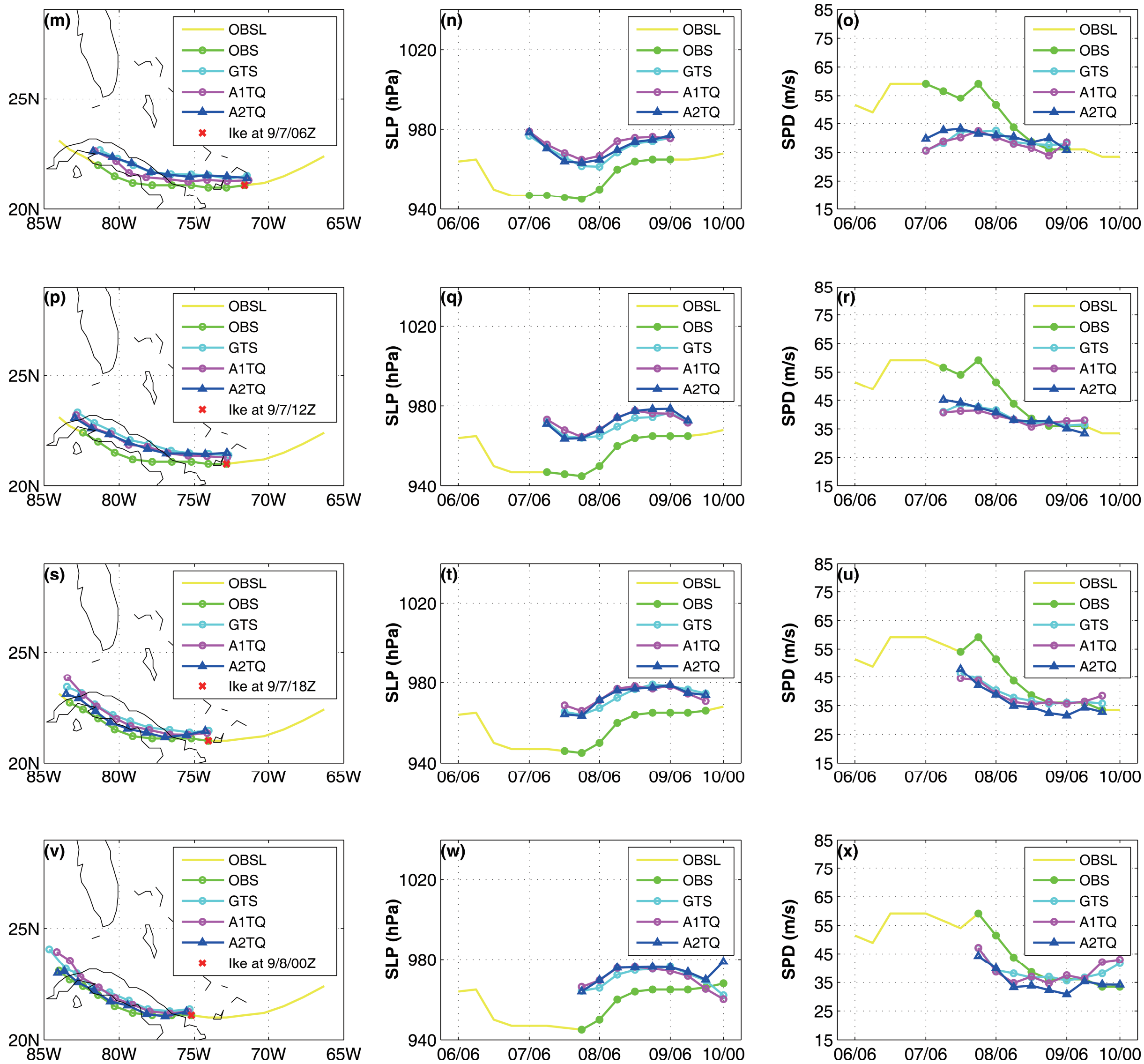

Fig. 2. (Continued.)

for the subsequent assimilation experiments, while the profiles below 700 hPa and above 200 hPa were not assimilated due to the larger biases.

Although no radiosonde observation was available to validate the AIRS profiles during the two hurricane periods, the evaluation results of the SciSup data compared against the ECMWF analysis are consistent with the validation studies carried out by Pu and Zhang (2010) and Miyoshi and Kunii (2012).

3. Numerical configuration and experiments

Based on the availability of the two types of AIRS sounding retrievals, a series of data assimilation and forecast experiments for two devastating hurricanes, Ike (2008) and Irene (2011), was conducted to investigate the impact of assimilating AIRS sounding retrievals on the forecasts of strong hurricanes.

3.1. *Hurricane cases*

Ike originated from a well-defined tropical wave on 28 August 2008. By 06 September, Ike had become a strong hurricane with deep convection redeveloping over its northern semicircle, and quickly returned to a strong hurricane (category 4) status by 1800 UTC that day. The center of Ike passed just south of the Turks and Caicos Islands at around 0600 UTC 07 September, with a minimum central sea-level pressure (SLP) of 947 hPa and a maximum low-level wind speed (SPD) of 59.2 m s^{-1} (i.e., 115 kt). Ike then weakened slightly before making landfall on Great Inagua Island in the southeastern Bahamas at around 1300 UTC 07 September. It restrengthened once again with an SLP of 945 hPa and SPD of 59.2 m s^{-1} by 0000 UTC 08 September. Ike made landfall at that intensity about two hours later in the early morning of 08 September and then gradually lost strength. As a long-lived hurricane, Ike and its related storm surge caused extensive damage along its path and during its four landfalls

(Berg, 2009).

Irene originated from a vigorous tropical wave in August 2011. It became a hurricane on 22 August and moved very close to the north coast of Hispaniola on 23 August. Irene moved away early on 24 August as a category 3 hurricane with a peak intensity of SPD 54 m s^{-1} (i.e., 105 kts) and an SLP of 957 hPa at 1200 UTC 24 August. It weakened slightly at around 0000 UTC 25 August and reached the Abaco Is-

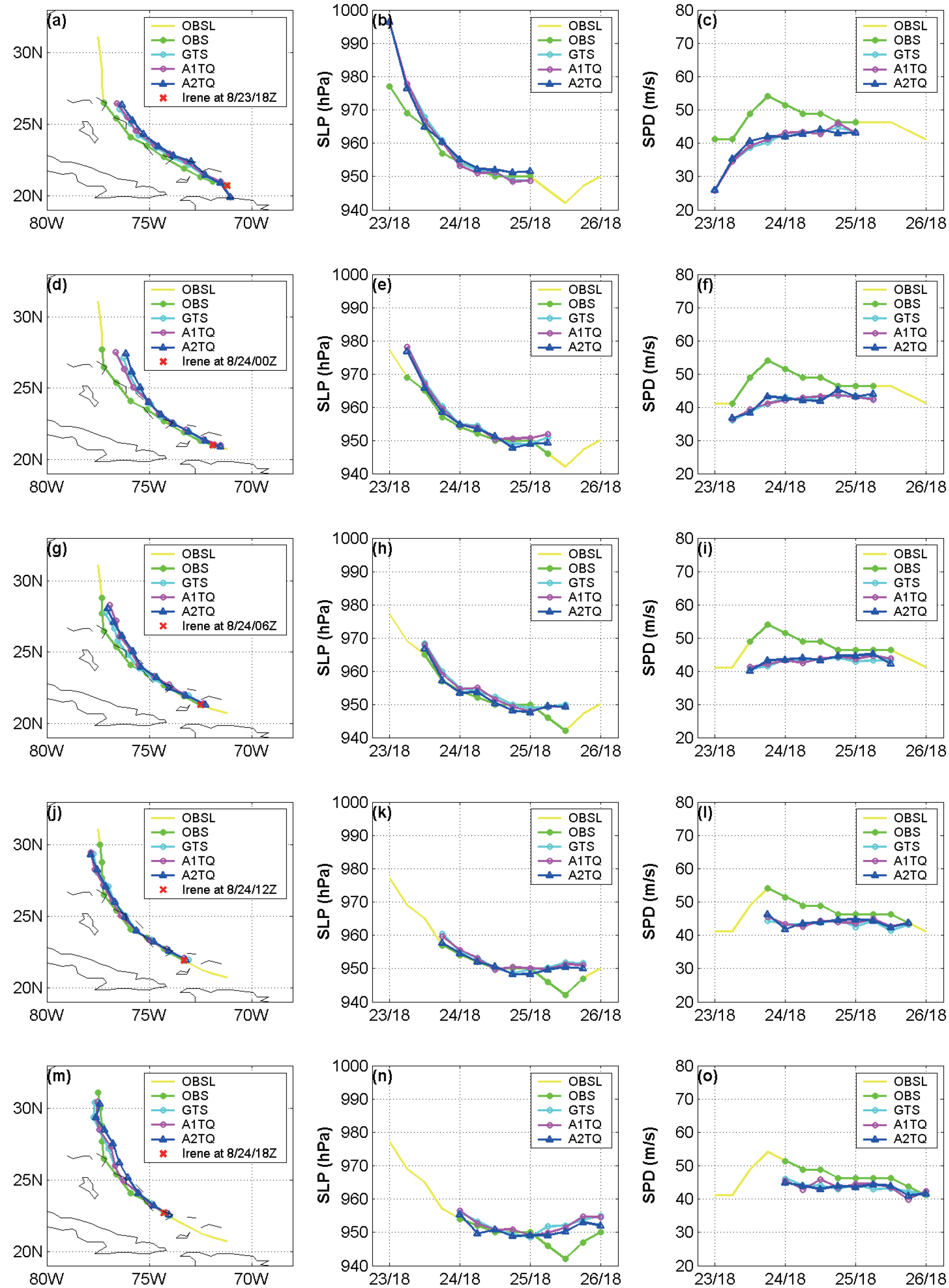

Fig. 3. As in Fig. 2, except for Hurricane Irene (2011) during 23–26 August 2011.

lands at around 1800 UTC 25 August with decreasing winds, but its SLP continued to fall to 942 hPa by 0600 UTC 26 August. It maintained hurricane strength for another two days and caused widespread damage across a large portion of the eastern United States (Avila and Cangialosi, 2011).

3.2. *Model and assimilation methodology*

The Advanced Research version of the WRF and its 3DVAR system (version 3.2.1) were applied for the numerical simulations in both cases. WRF is a fully compressible and non-hydrostatic model, with a terrain-following hydrostatic pressure coordinate and Arakawa C-grid staggering. The model uses the Runge–Kutta 2nd- and 3rd-order time integration schemes and 2nd- to 6th-order advection schemes in both the horizontal and vertical direction. 3DVAR assimilated the conventional observations and the AIRS profiles, and then recombined them with the background (i.e., the NWP model state) to produce an optimal analysis of the true state as the initial conditions for the WRF forecast (Skamarock et al., 2008; Barker et al., 2012).

National Centers for Environmental Prediction (NCEP) operational final analysis (FNL) data with $1.0^\circ \times 1.0^\circ$ resolution (ds083.2 from http://dss.ucar.edu/) were used to provide the background at the beginning cycle of the assimilation when the WRF output was not available. They were also used as the boundary conditions every six hours during the forecast period. The "gen_be" utility in the WRF-3DVAR package was used to generate domain-specific climatological estimates of background error covariance (***B***) matrices. Known as the NMC (National Meteorological Center; now known as NCEP) method (Parrish and Derber, 1992), it is based on the differences of 24- and 12-h forecasts (valid at the same time) initialized at 0000 UTC and 1200 UTC (or 0600 UTC and 1800 UTC) for a whole month. In Ike's case, the ***B*** matrix was calculated from 07 August 2008 to 06 September 2008; while in Irene's case, it was calculated from 22 July 2011 to 21 August 2011. There was no additional tuning work on the ***B*** calculation in this study. According to the validation results reported in section 2, the AIRS temperature STD error was set to 1 K for 200–700 hPa, and the relative STD error of the specific humidity was set to 10% of its absolute value for 300–700 hPa and 20% for 200–300 hPa. The STD errors of conventional observations were assumed as 1 K for temperature at all pressure levels, 15% for relative humidity

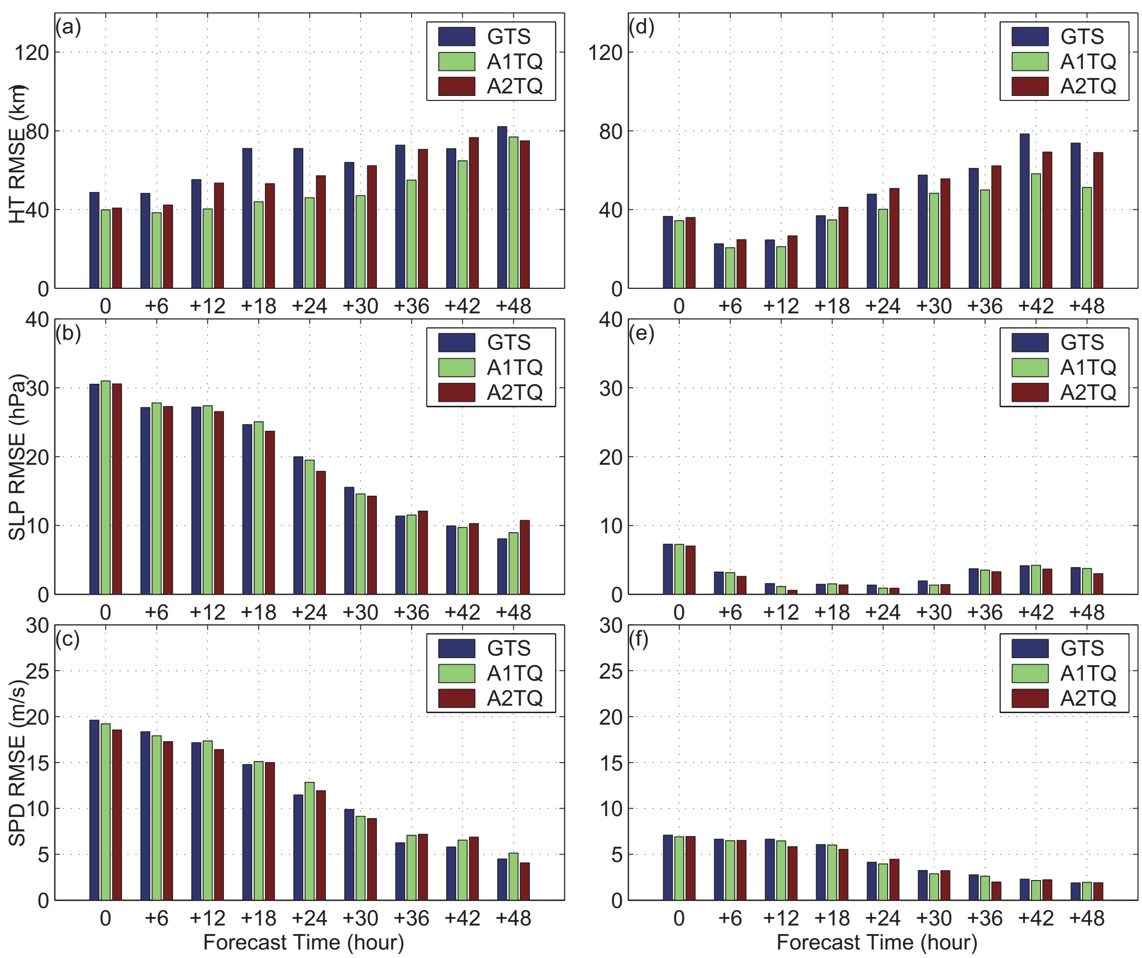

Fig. 4. RMSEs for hurricanes (a–c) Ike (2008) and (d–f) Irene (2011). The *y*-coordinate is the RMSE for HT, SLP and SPD, respectively, while the *x*-coordinate denotes the forecast time from 0 h (analysis), 6 h, 12 h, 18 h, 24 h, 30 h, 36 h, 42 h to 48 h.

at 1000 hPa, and 10% at all other pressure levels. Besides, the observational error covariance matrices were determined and treated as diagonal matrices. The conventional observations and AIRS temperature and moisture data were excluded if their differences from the model background were greater than five times the assumed observational errors.

3.3. *Assimilation and forecast experiments*

A single domain with a 12-km horizontal resolution was used in the numerical experiments. The model set up 35 vertical levels from the surface to the top at 50 hPa with higher resolution in the planetary boundary layer (PBL). The major model physics options included the Yonsei University (YSU) PBL parameterization scheme (Hong et al., 2006), the Rapid Radiative Transfer Model for General circulation model (RRTMG) longwave and shortwave atmospheric radiation schemes (Clough et al., 2005; Iacono et al., 2008; Morcrette et al., 2008), and the new Kain–Fritsch cumulus parameterization scheme (Kain, 2004). The assimilation time window was set to be $\pm$60 minutes and no bogus vortex was used in the initial conditions.

In Ike's case (2008), the domain consisted of 480×240 grid points and was centered at (20°N, 70°W). There were eight assimilation cycles starting at 0600 UTC 06 September and ending at 0000 UTC 08 September with intervals of 6 h. Apart from the first assimilation cycle, the WRF short-range (6 h) forecast was used as the background in the remaining assimilation cycles. In addition, there was a 48 h forecast following in each assimilation cycle. In Irene's case (2011), the configuration was similar, except that the domain center was located at (21°N, 70°W) with 480×300 grid points and five assimilation cycles were conducted starting at 1800 UTC 23 August and ending at 1800 UTC 24 August.

Conventional observation data from the global telecommunication system (GTS) were available at each assimilation cycle, including reports of surface observations from land and ocean (ship) stations, aircraft, ocean buoys, wind profiler, aerodrome, upper-level pressure and surface radiosondes, thickness observation, ground-based GPS precipitable water, space-based GPS refractivity, ocean surface wind data from Quick Scatterometer (QuikSCAT) satellite and geostationary satellite-derived atmospheric motion vectors. The AIRS-retrieved temperature (T) and moisture (Q) profiles were available only at 0600 UTC and 1800 UTC from either the SFOV or the SciSup products. Generally, conventional observations have difficulty in describing the vertical atmospheric T and Q structures over an open ocean with few radiosondes; while the AIRS sounding retrievals add more horizontal and vertical T and Q information. To investigate the impact of assimilating different AIRS sounding retrievals on hurricane forecast skills, GTS observations with and without AIRS retrievals were assimilated. For each hurricane case, a series of eight numerical experiments was designed, as summarized in Table 1, including (1) a control experiment without assimilation of AIRS data, i.e., the GTS experiment; (2) assimilation of SFOV's T profiles in addition to GTS data, i.e., the A1T experiment; (3) assimilation of SFOV's T and Q profiles in addition to GTS data, i.e., the A1TQ experiment; (4) assimilation of SciSup's T profiles in addition to GTS data, i.e., the A2T experiment; (5) assimilation of SciSup's T and Q profiles in addition to GTS data, i.e., the A2TQ experiment; (6) assimilation of SFOV's matching T profiles in addition to GTS data, i.e., the A1TM experiment; (7) assimilation of SciSup's matching T profiles in addition to GTS data, i.e., the A2TM experiment. According to the quality control described in section 2, the SFOV profiles were available in clear skies, while the SciSup profiles included some non-precipitation cloudy retrievals. In the A1T, A1TQ, A2T and A2TQ experiments, all the available best SFOV and SciSup retrievals between 200 hPa and 700 hPa were assimilated. In the A1TM and A2TM experiments, the SFOV and SciSup data counts were matched at the same location after their individual stringent quality control from A1T and A2T. Thus, these matching profiles were strictly over clear skies.

Table 1. Numerical experiments designed for each hurricane study.

Experiment	Assimilated observations
GTS	GTS only
A1T	GTS plus SFOV's T
A1TQ	GTS plus SFOV's T and Q
A2T	GTS plus SciSup's T
A2TQ	GTS plus SciSup's T and Q
A1TM	GTS plus SFOV's matching T
A2TM	GTS plus SciSup's matching T

4. Impact verification

Our preliminary assessment of the impact of AIRS assimilation focused on the following aspects. Firstly, for every 6 h interval, the hurricane track (HT), minimum central SLP, and maximum SPD were validated against the best track record from observational hurricane reports (Berg, 2009; Avila and Cangialosi, 2011). Secondly, the water vapor distribution with regard to the TPW was validated against the TPW reference from the Advanced Microwave Scanning Radiometer for EOS (AMSR-E) at 21 km resolution over the ocean (Wentz and Meissner, 2004, 2007). Thirdly, the surface rain forecast was compared with the rainfall data from Tropical Rainfall Measuring Mission (TRMM) data, version 7 (http://trmm.gsfc.nasa.gov/) at 4–5 km horizontal resolution.

4.1. *HT, SLP and SPD*

Figures 2 and 3 show the 48 h forecasts of HT, SLP and SPD from the GTS, A1TQ and A2TQ experiments against the best hurricane record. In both hurricane cases, the GTS experiments showed capable skill in short-range (6–12 h) HT forecasts, with especially good skill in the case of Irene. Interestingly, Ike's restrengthened SLP in the early part of 08 September 2008 was reproduced well by the NWP experiments, while Irene's restrengthened SLP in the early part of 26 August 2011 was not. When additional AIRS data (either SFOV or SciSup) were assimilated at 0600 and 1800 UTC (e.g., A1TQ and A2TQ), the forecasted HT biases were

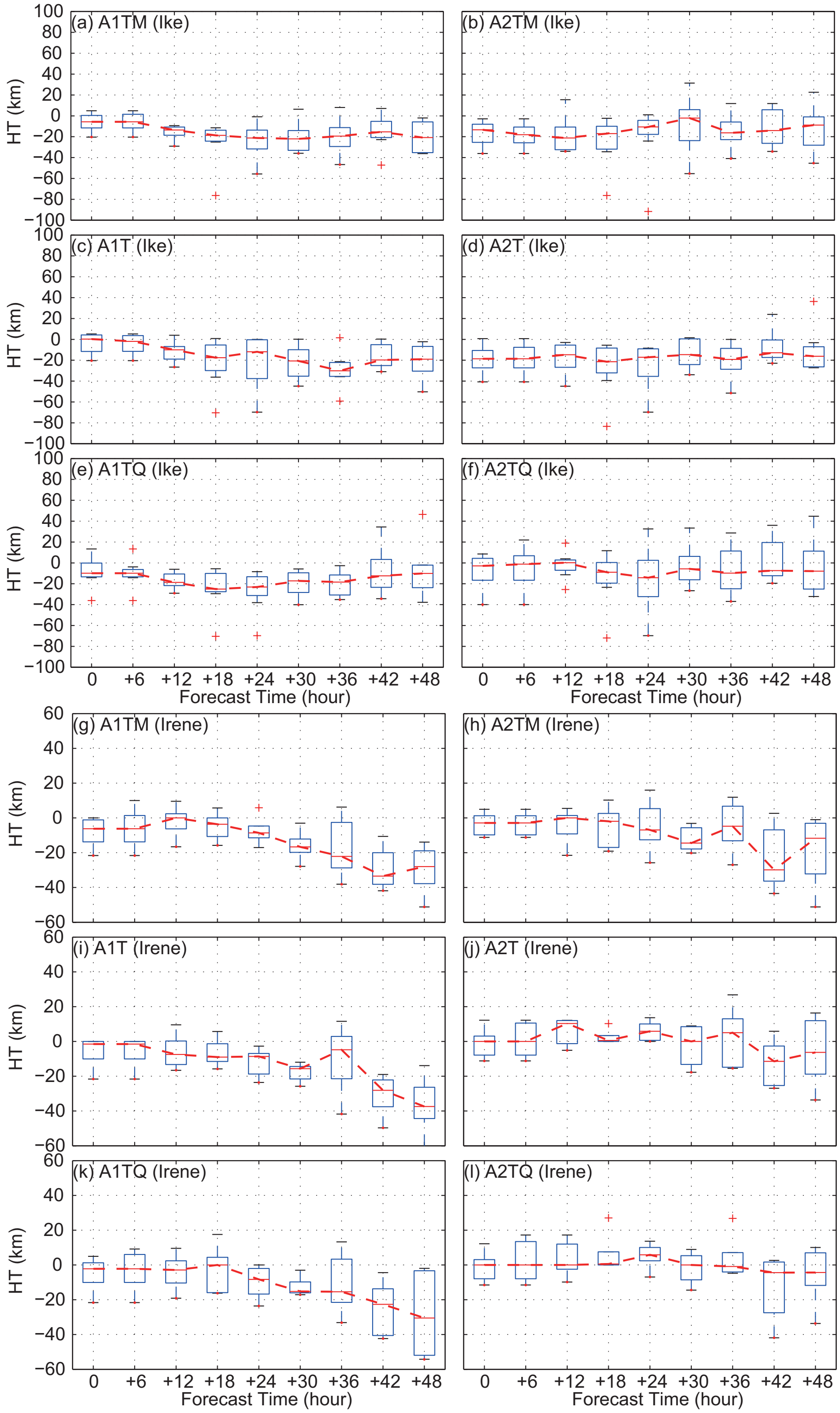

Fig. 5. Box plots of the HT error difference (AIRS minus GTS). The *x*-coordinate denotes the forecast time from 0 h (analysis), 6 h, 12 h, 18 h, 24 h, 30 h, 36 h, 42 h, to 48 h. The *y*-coordinate is the error deviation between each AIRS experiment (listed in Table 1) and the GTS experiment. In each box plot, the upper and lower ends of the column are drawn at the quartiles of $q_{0.75}$ and $q_{0.25}$, and the red bar through the box is drawn at the median ($q_{0.5}$). The whiskers extend from the quartiles to the maximum and minimum data values. The outliers are data beyond the ends of the whiskers. If there are no data outside the whisker, a dot is placed at the bottom whisker.

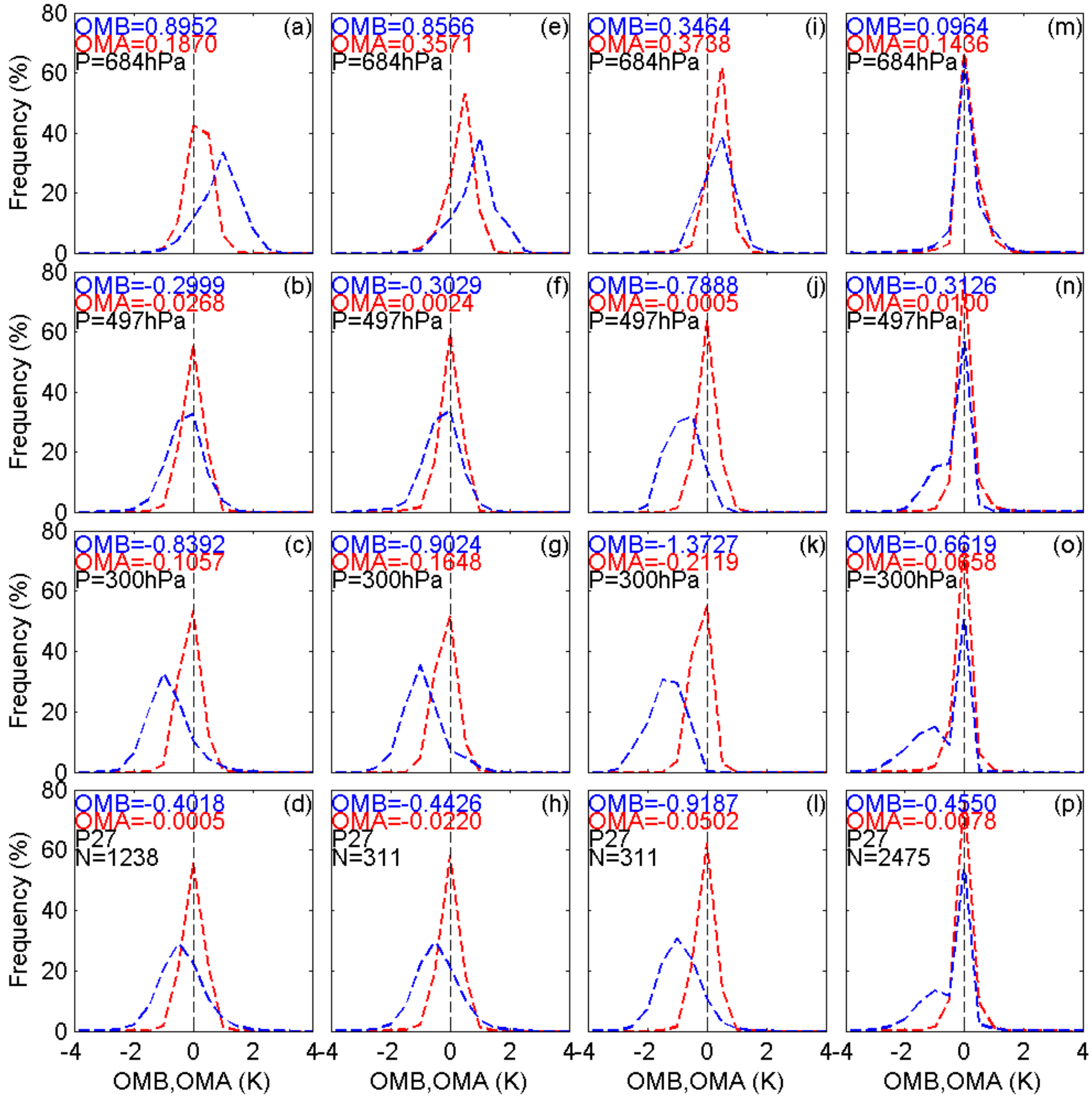

Fig. 6. Temperature innovations (OMB) and analysis residuals (OMA) from the (a–d) A1TQ, (e–h) A1TM, (i–j) A2TM, and (k–p) A2TQ experiments at different vertical levels in the first assimilation cycle in the case of Ike (2008). P27 is the layer mean of 200–700 hPa. *N* represents the assimilated AIRS temperature counts.

reduced largely in the case of Ike (Fig. 2), and the biases remained small in the case of Irene (Fig. 3). Meanwhile, the forecasted intensity (SLP and SPD) biases showed little change among GTS, A1TQ and A2TQ in either case. Figure 4 shows the root-mean-square errors (RMSEs) of the GTS, A1TQ and A2TQ experiments. The averaged RMSEs from the 0–48 h forecast experiments were approximately 60 km for HT, 15 hPa for SLP, and 10 m s^{-1} for SPD in Ike's case, and they were 50 km, 4 hPa, and 4 m s^{-1} in Irene's case. This result reinforced the finding that the forecast skill in the case of Irene (2011) was statistically better than that in the case of Ike (2008). It was also found that the AIRS data assimilation showed general improvement in longer-lead HT forecasts compared with the GTS experiments. Specifically, adding SFOV assimilation in the A1TQ experiments produced noticeable improvement in the HT forecast (an approximate 10–20 km error reduction in the 24–48 h forecast in both cases), while adding SciSup assimilation in the A2TQ experiment produced less improvement (Figs. 4a and d). Meanwhile, neither showed significant improvement in terms of hurricane intensity (SLP and SPD) forecasts. Figure 5 shows box plots of the HT error difference between each AIRS experiment and the GTS experiment (i.e., AIRS minus GTS). The negative value represents positive improvement of error reduction when adding AIRS in the assimilation. Comparisons between experiments of assimilating AIRS temperature profiles with and without its moisture profiles (A1TQ vs A1T, and A2TQ vs A2T) showed similar trends during the

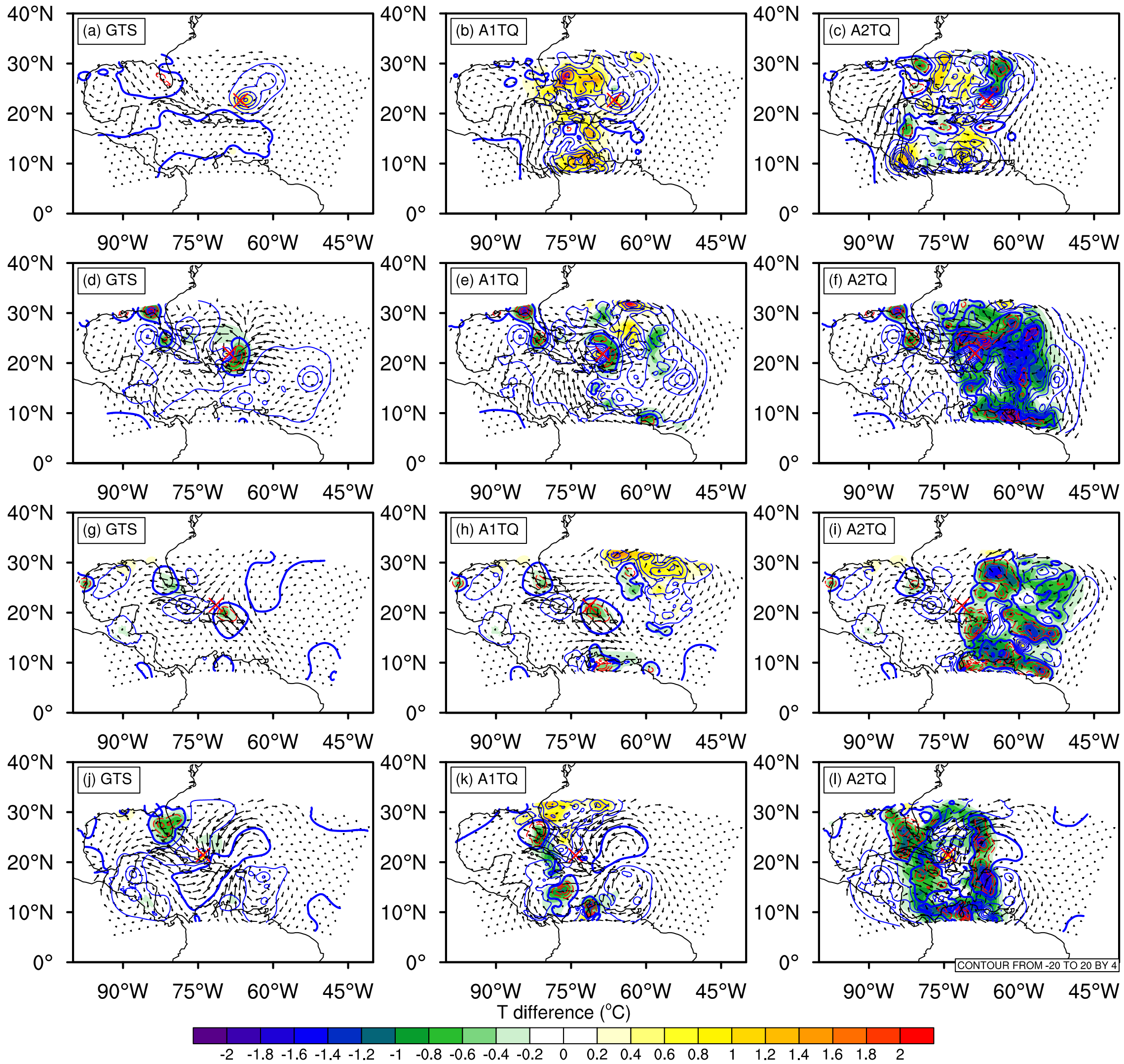

Fig. 7. Analysis increments of 700 hPa temperature (shaded, units: °C), 500 hPa geopotential height (contours, units: gpm), and 500 hPa wind vector (units: m s^{-1}) from the GTS, A1TQ and A2TQ experiments in the case of Ike (2008). Panels (a–c) represent the assimilation cycle at 0600 UTC 6 September 2008, (d–f) at 1800 UTC 06 September 2008, (g–i) at 0600 UTC 7 September 2008, and (j–l) at 1800 UTC 7 September 2008. The red cross shows the location of Ike (2008). The blue solid line indicates positive values, and the red dashed line indicates negative values. The contour interval is 4 gpm, with the blue bold line having a value of zero in the contour.

forecast time. The results indicated that the impact of assimilating AIRS temperature profiles exceeded that of moisture profiles with respect to the positive HT improvement using the current 3DVAR methodology. Although the matching AIRS data assimilated in the A1TM and A2TM reduced to a quarter or even less compared to those in the A1T and A2T experiments, the HT results of the A1TM and A2TM experiments showed a similar range of improvement to that of the A1T and A2T experiments in both hurricane cases.

Figure 6 shows the temperature innovations (i.e., OMB, the discrepancies between AIRS data and the background state) and analysis residuals (i.e., OMA, the discrepancies between AIRS data and 3DVAR analysis) from the A1TM, A1TQ, A2TM and A2TQ experiments at different vertical levels. When all SFOV profiles were assimilated, the A1TQ experiment showed a warm signal in the lower levels (OMB>0 in Fig. 6a) and a cold signal in the upper levels (OMB<0 in Figs. 6b and c). This was consistent with the previous AIRS evaluation results using AIRS sounding retrievals, reported in section 2 (Figs. 1a–d). The A2TQ experiment showed a second cold peak in the upper levels that made the mean profile cold (OMB<0 in Figs. 6n–p). When the matching SFOV and SciSup data over clear skies were assimilated, the A1TM and A2TM experiments showed a similar warm OMB at 684 hPa (Figs. 6e and i) and a cold OMB in the other upper levels (Figs. 6f, g, i and k). The OMB differences between the A2TM and A2TQ experiments were probably caused by those cloudy profiles that were not included after matching SciSup with SFOV. After the assimilation by 3DVAR, the OMA showed a better distribution than that of

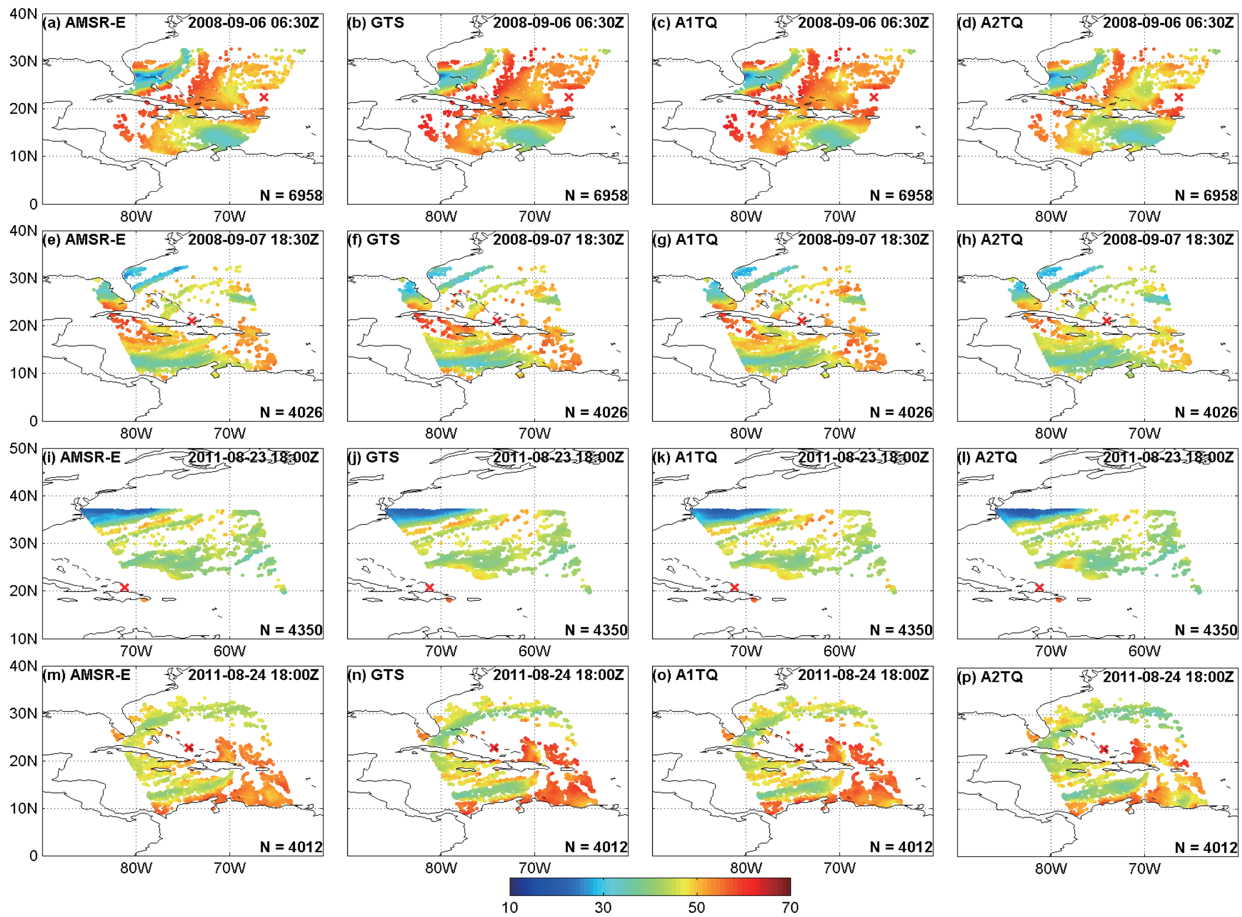

Fig. 8. TPW spatial distribution against AMSR-E reference data during hurricanes Ike (2008) and Irene (2011). *N* is the sampling data count at each time. The red cross shows the hurricane's location.

OMB in all levels, with the A1TM and A2TM experiments showing slightly warmer results (by about 0.2 °C) than the A1TQ and A2TQ experiments at 684 hPa.

Figure 7 shows the analysis increments (analysis minus background) of the assimilation cycles from the GTS, A1TQ and A2TQ experiments for the case of Ike when AIRS data were assimilated, including increments of 700 hPa temperature (T), 500 hPa geopotential height (GH), and 500 hPa wind vector. It was found that the T increments due to AIRS assimilation could induce the GH increments through thermodynamic adjustment, thus having an impact on the large-scale steering flow in the mid troposphere to adjust the hurricane track. With different types and amounts of AIRS data being assimilated in the A1TQ and A2TQ experiments at different times, the T increments showed different warming or cooling environments compared with the GTS experiment. When warmer AIRS data (mostly from SFOV) were assimilated, the GH tended to increase; while when colder AIRS (from SciSup) were assimilated, the GH tended to decrease. Consequently, the steering flows leading the hurricane track were different in the A1TQ and A2TQ experiments. Similar results were found in the case of Irene. However, the hurricane's SLP and SPD showed insignificant change to the environmental GH variation. One possible reason is that, apart from the steering flow, other factors may also contribute to a hurricane's movement and intensity variations in different aspects, such as the upper level jet, the sea surface temperature, the change of vertical wind shear, the inner hurricane dynamics, and the interactions between the large-scale environment and the hurricane (Emanuel, 1999; Roy and Kovordányi, 2012; Wu et al., 2012). Therefore, hurricane forecasts, especially intensity forecast, have represented a major challenge over the past decade and deserve further study (National Hurricane Center, 2013, http://www.nhc.noaa.gov/verification/).

4.2. *TPW*

The AMSR-E TPW over the ocean has been used as the reference to validate the water vapor distribution in many studies (e.g., Fetzer et al., 2006; Lee et al., 2014) because AMSR-E has the advantage of a constant viewing angle and sensitivity to cloud liquid water and precipitation (Kawanishi et al., 2003), and its microwave frequencies are not affected by non-precipitating clouds (O'Neill et al., 2005). The clear-sky TPW from AMSR-E was selected as the reference, and the WRF-forecasted TPW was collocated with it within a distance of 8 km and a time interval of 15–30 min. As shown

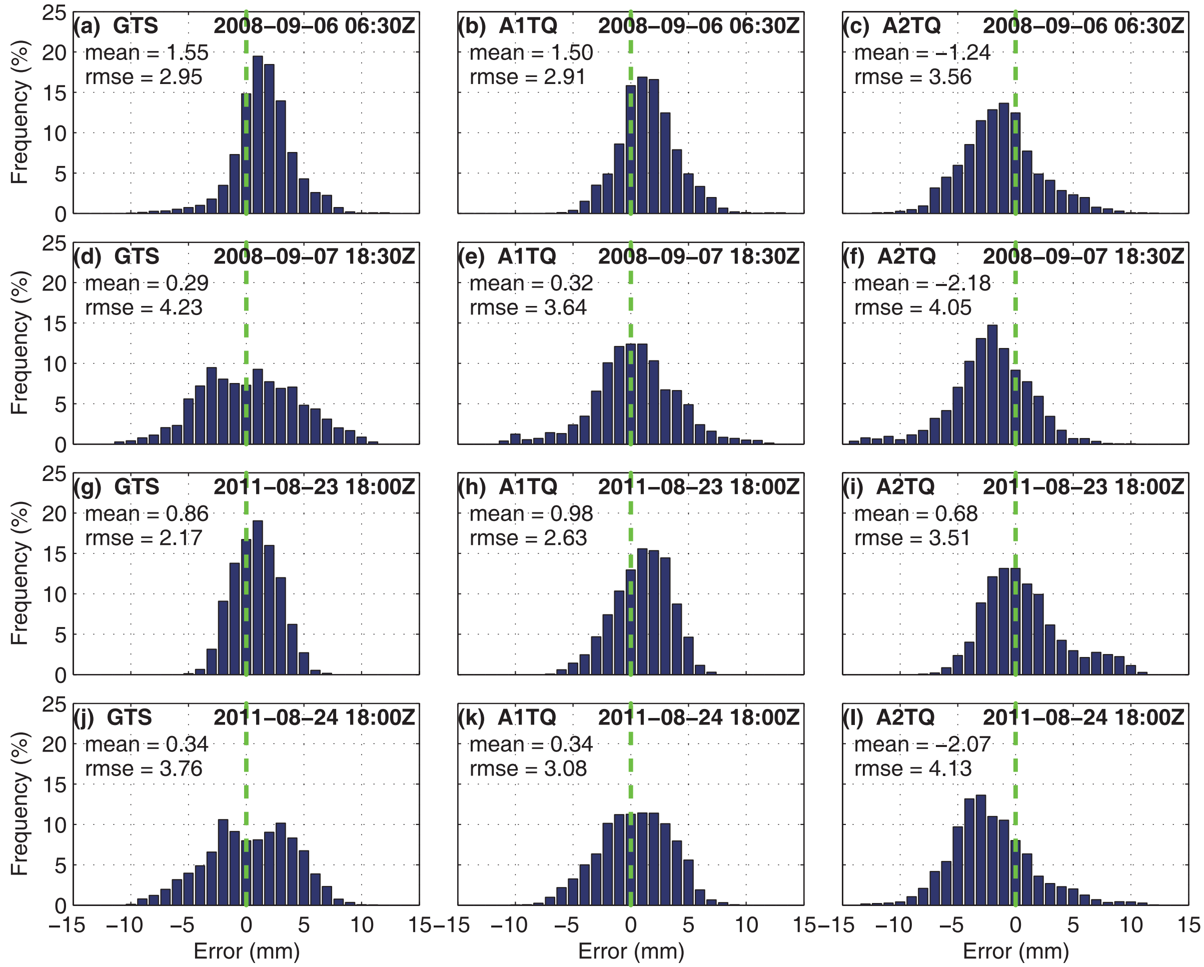

Fig. 9. Histograms of forecasted TPW error distributions against AMSR-E TPW at four selected times as in Fig. 8.

in Fig. 8, all the forecasted TPW showed consistent structures of dry and wet bands surrounding the hurricane compared with the AMSR-E, except in the A2TQ experiment, which was a bit drier. Figure 9 shows the forecasted TPW errors at the four matching time slots in Fig. 8. In both hurricane cases, when SFOV's Q was assimilated in the first cycle, the mean TPW errors of A1TQ were similar to those of GTS (Figs. 9a, b and g, h), while the mean TPW errors of A2TQ were the smallest (Figs. 9c and i). In Ike's case, during the period from 0630 UTC 06 September to 1830 UTC 07 September, the RMSE went from 2.95 mm to 4.23 mm in the GTS (ΔRMSE = 1.28 mm), from 2.91 mm to 3.64 mm in the A1TQ (ΔRMSE = 0.73 mm), and from 3.56 mm to 4.05 mm in the A2TQ (ΔRMSE = 0.49 mm) experiment. In Irene's case, during the period from 1800 UTC 23 August to 1800 UTC 24 August, the RMSE went from 2.17 mm to 3.76 mm in the GTS (ΔRMSE = 1.59 mm), from 2.63 mm to 3.06 mm in the A1TQ (ΔRMSE = 0.43 mm), and from 3.51 mm to 4.13 mm in the A2TQ (ΔRMSE = 0.62 mm) experiment. This result showed that the continuous cycling of AIRS Q assimilation was able to constrain the RMSE a bit better than that without AIRS Q assimilation. Besides, the underestimation of TPW in the A2TQ experiment was possibly due to the impact of assimilating SciSup's Q profiles, which were drier than SFOV's Q profiles in this study. These results imply that, although the moisture profiles showed little direct impact on hurricane track and intensity forecasts by WRF-3DVAR, they may contribute to the hurricane moisture environment forecast.

4.3. *Rainfall*

TRMM was launched in 1997 to measure global tropical rainfall (Simpson et al., 1988; Kummerow et al., 1998). To capture the rain structure, the combined data of surface rain from the TRMM microwave imager (TMI), as in the 2A12 product, and precipitation radar (PR), as in the 2A25 product, were used as the reference.

Figure 10 represents the results of rain distribution. TRMM showed more detailed and stronger convective rainfall structure, with a larger peak value (60–130 mm h^{-1}) at its high horizontal resolution (i.e., 4–5 km). Compared with TRMM, the WRF forecasts of 1 h, 17 h and 48 h captured the structure of Ike's rain band around the hurricane eyes generally well in the GTS, A1TQ and A2TQ experiments (Figs. 10a–l), with similar patterns within the 24 h forecast time (Figs. 10b–d and f–h). When the forecast time was extended

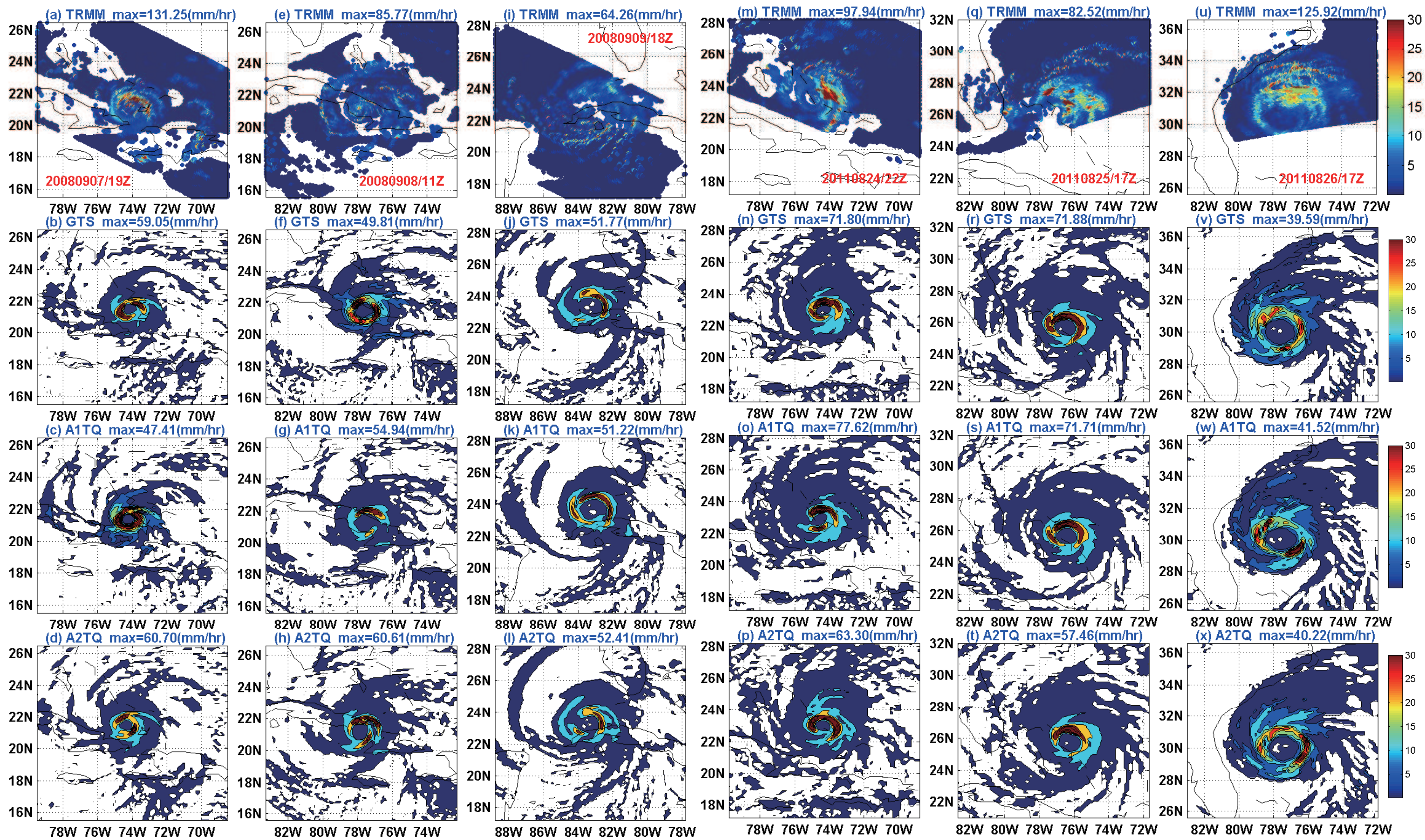

Fig. 10. Precipitation distribution against TRMM (Units: mm h^{-1}). The WRF forecasts started in the last AIRS assimilation cycle at 1800 UTC 07 September 2008 for Ike and 1800 UTC 24 August 2011 for Irene.

to 48 h, deeper convection with heavier and an almost closed-circle rainfall band appeared in Ike's eyewall region in A1TQ (Fig. 10k), while the rainfall bands were a bit weaker in the GTS and A2TQ experiments (Figs. 10j and l). Similar results were found for the WRF forecasts of 4 h, 23 h and 47 h in Irene's case (Figs. 10m–x), except that when the forecast time approached 47 h, the regions of deep convection were slightly different in different experiments (Figs. 10u–x) and there was a second rain band in the north (near 34°N) in A1TQ that fitted the TRMM results (Fig. 10w). This weak rain band was located about 1° south in the GTS and A2TQ experiments (Figs. 10v and x). These results indicate that the effect of AIRS moisture assimilation on rainfall tends to be a long-term one (about 48 h).

5. Summary and discussion

In this study, AIRS temperature and moisture sounding retrievals from the UW/CIMSS (SFOV) and AIRS Science Team (SciSup) products were evaluated with ECMWF analysis data, and then assimilated using a regional WRF-3DVAR system to investigate their impact on hurricane forecasts. Different sets of cycling assimilation and forecast experiments were conducted for two hurricane cases, Ike (2008) and Irene (2011).

During the two hurricane periods, AIRS validation results showed a mean bias of 1 K for both AIRS temperature profiles under 200 hPa, and a mean bias within 1 g kg^{-1} for the moisture profiles at 700 hPa. Hence, the SFOV and SciSup products of best quality between 200 hPa and 700 hPa were assimilated directly in the NWP impact study.

Numerical experiment results showed an overall improvement in the longer-lead track forecasts by assimilating additional AIRS sounding retrievals, especially when SFOV temperature profiles were assimilated. The analysis increments and temperature innovations indicated that the HT variation due to assimilating the AIRS temperature profiles was related to the thermodynamic adjustment of the environment's GH, and thus the steering flow that guided the hurricane movement was changed accordingly.

The hurricane intensity forecasts in terms of SLP and SPD showed little change when either SFOV or SciSup profiles were assimilated. Although assimilating either type of moisture profile had little impact on the HT, SLP and SPD forecasts, a cycling assimilation of SFOV moisture profiles was found to constrain the forecasted TPW error in this study. As for the rainfall, the WRF model with AIRS cycling assimilation generally captured reasonable rain structures as the forecast time extended, and stronger rain bands were found in the A1TQ experiment (with SFOV assimilation) in longer-lead forecasts than those in the GTS (without AIRS assimilation) and A2TQ (with SciSup assimilation) experiment for both hurricanes.

Further extensions to this study will include: (1) assimilating more clear-sky and cloudy retrievals, especially those under the 700 hPa level, and conducting bias correction if these data are evaluated to possess large biases; (2) updating the 3DVAR method (which is not sensitive to moisture assimilation) with an advanced hybrid-3DVAR method; (3) assimilating additional satellite data (e.g., AMSU-A) in the regional NWP; and (4) analyzing more case studies, such as typhoons over the northwest Pacific Ocean.

Acknowledgements. The authors appreciate all the helpful comments from the reviewers. In terms of model support, we would like to thank the WRF model and WRFDA teams. For AIRS data support, we would like to thank UW/CIMSS and the AIRS Science team. We also thank the European Center for Medium Range Forecasting group and the National Centers for Environmental Prediction for providing data used in this study. This work was supported by the National Natural Science Foundation of China (Grant No. 41305089), the National Oceanic and Atmospheric Administration (Grant No. NA10NES4400013), and the Public Industry-specific Fund for Meteorology (Grant No. GYHY201406011). The views, opinions, and findings contained in this publication are those of the authors and should not be construed as an official government position, policy, or decision.

REFERENCES

Atlas, R., 2005: The impact of AIRS data on weather prediction. *Proc. SPIE 5806*, Algorithms and Technologies for Multispectral, Hyperspectral, and Ultraspectral Imagery XI, 599 (July 13, 2005), doi: 10.1117/12.602540.

Aumann, H. H., and Coauthors, 2003: AIRS/AMSU/HSB on the Aqua mission: Design, science objectives, data products, and processing systems. *IEEE Trans. Geosci. Remote Sens.*, **41**(2), 253–264, doi: 10.1109/TGRS.2002.808356.

Avila, L. A., and J. Cangialosi, 2011: Tropical Cyclone Report — Hurricane Irene (AL092011). National Hurricane Center, 45 pp. [Available online at http://www.nhc.noaa.gov/2011atlan.shtml.]

Barker, D., and Coauthors, 2012: The weather research and forecasting model's community variational/ensemble data assimilation system: WRFDA. *Bull. Amer. Meteor. Soc.*, **93**, 831–843.

Berg, R., 2009: Tropical Cyclone Report—Hurricane Ike (AL 092008). National Hurricane Center, 55 pp. [Available online at http://www.nhc.noaa.gov/2008atlan.shtml.]

Chahine, M. T., and Coauthors, 2006: AIRS: Improving weather forecasting and providing new data on greenhouse gases. *Bull. Amer. Meteor. Soc.*, **87**, 911–926. doi: 10.1175/BAMS-87-7-911.

Chen, S.-H., Z. Zhao, J. S. Haase, A. Chen, and F. Vandenberghe, 2008: A study of the characteristics and assimilation of retrieved MODIS total precipitable water data in severe weather simulations. *Mon. Wea. Rev.*, **136**, 3608–3628.

Clough, S. A., M. W. Shephard, E. J. Mlawer, J. S. Delamere, M. J. Iacono, K. Cady-Pereira, S. Boukabara, and P. D. Brown, 2005: Atmospheric radiative transfer modeling: A summary of the AER codes. *Journal of Quantitative Spectroscopy and Radiative Transfer*, **91**, 233–244.

Derber, J. C., and W.-S. Wu, 1998: The use of TOVS cloud-cleared radiances in the NCEP SSI analysis system. *Mon. Wea. Rev.*, **126**, 2287–2299.

Divakarla, M., G. C. D. Barnet, M. D. Goldberg, L. M. McMillin, E. Maddy, W. Wolf, L. Zhou, and X. Liu, 2006: Validation of atmospheric infrared sounder temperature and water vapor retrievals with matched radiosonde measurements and forecasts. *J. Geophys. Res.*, **111**, D09S15, doi: 10.1029/2005JD006116.

Emanuel, K. A., 1999: Thermodynamic control of hurricane intensity. *Nature*, **401**, 665–669.

Fetzer, E. J., B. H. Lambrigtsen, A. Eldering, H. H. Aumann, and M. T. Chahine, 2006: Biases in total precipitable water vapor climatologies from Atmospheric Infrared Sounder and Advanced Microwave Scanning Radiometer. *J. Geophys. Res.*, **111**, DS09S16, doi: 10.1029/2005JD006598.

Hong, S.-Y., Y. Noh, and J. Dudhia, 2006: A new vertical diffusion package with an explicit treatment of entrainment processes. *Mon. Wea. Rev.*, **134**, 2318–2341.

Iacono, M. J., J. S. Delamere, E. J. Mlawer, M. W. Shephard, S. A. Clough, and W. D. Collins, 2008: Radiative forcing by long-lived greenhouse gases: Calculations with the AER radiative transfer models. *J. Geophys. Res.*, **113**, D13103, doi: 10.1029/2008JD009944.

Jedlovec, G. J., S. H. Chou, B. T. Zavodsky, and W. Lapenta, 2006: The use of error estimates with AIRS profiles to improve short-term weather forecasts. *Proc. SPIE. 6233*, Algorithms and Technologies for Multispectral, Hyperspectral, and Ultraspectral Imagery XII, 62331B (May 05, 2006), doi: 10.1117/12.665724.

Kain, J. S., 2004: The Kain–Fritsch convective parameterization: An update. *J. Appl. Meteor.*, **43**, 170–181.

Kawanishi, T., and Coauthors, 2003: The Advanced Microwave Scanning Radiometer for the Earth Observing System (AMSR-E), NASDA's contribution to the EOS for global energy and water cycle studies. *IEEE Trans. Geosci. Remote Sens.*, **41**, 184–194.

Kummerow, C., W. Barnes, T. Kozu, J. Shiue, and J. Simpson, 1998: The tropical rainfall measuring mission (TRMM) sensor package. *J. Atmos. Oceanic Technol.*, **15**, 809–817.

Kwon, E.-H., J. Li, J. Li, B. J. Sohn, and E. Weisz, 2012: Use of total precipitable water classification of a priori error and quality control in atmospheric temperature and water vapor sounding retrieval. *Adv. Atmos. Sci.*, **29**(2), 263–273, doi: 10.1007/s00376-011-1119-z.

Leidner, S. M., L. Isaksen, and R. N. Hoffman, 2003: Impact of NSCAT winds on tropical cyclones in the ECMWF 4DVAR assimilation system. *Mon. Wea. Rev.*, **131**, 3–26.

Le Marshall, J., and Coauthors, 2006: Improving global analysis and forecasting with AIRS. *Bull. Amer. Meteor. Soc.*, **87**, 891–894.

Lee, Y.-K., Z. Li, J. Li, and T. Schmit, 2014: Evaluation of the GOES-R ABI LAP retrieval algorithm using the GOES-13 Sounder. *J. Atmos. Oceanic Tech.*, **31**, 3–19.

Li, J., and H.-L. Huang, 1999: Retrieval of atmospheric profiles from satellite sounder measurements by use of the discrepancy principle. *Appl. Opt.*, **38**, 916–923.

Li, J., and J. L. Li, 2008: Derivation of global hyperspectral resolution surface emissivity spectra from advanced infrared sounder radiance measurements. *Geophys. Res. Lett.*, **35**, L15807, doi: 10.1029/2008GL034559.

Li, J., and H. Liu, 2009: Improved hurricane track and intensity forecast using single field-of-view advanced IR sounding measurements. *Geophys. Res. Lett.*, **36**, L11813, doi: 10.1029/2009GL038285.

Li, J., W. Wolf, W. P. Menzel, W. Zhang, H.-L. Huang, and T. H. Achtor, 2000: Global soundings of the atmosphere from ATOVS measurements: The algorithm and validation. *J. Appl. Meteor.*, **39**, 1248–1268.

Li, J., W. P. Menzel, F. Sun, T. J. Schmit, and J. Gurka, 2004: AIRS sub-pixel cloud characterization using MODIS cloud products. *J. Appl. Meteor.*, **43**, 1083–1094.

Liu, H., and J. Li, 2010: An improvement in forecasting rapid intensification of typhoon Sinlaku (2008) using clear-sky full spatial resolution advanced IR soundings. *J. Appl. Meteor. Climatol.*, **49**, 821–827.

Lorenc, A. C., and Coauthors, 2000: The Met office global three-dimensional variational data assimilation scheme. *Quart. J. Roy. Meteor. Soc.*, **126**, 2991–3012.

McCarty, W., G. Jedlovec, and T. L. Miller, 2009: Impact of the assimilation of Atmospheric Infrared Sounder radiance measurements on short-term weather forecasts. *J. Geophys. Res.*, **114**, D18122, doi: 10.1029/2008JD011626.

Migliorini, S., 2012: On the equivalence between radiance and retrieval assimilation. *Mon. Wea. Rev.*, **140**, 258–265.

Migliorini, S., C. Piccolo, and C. Rodgers, 2008: Use of the information content in satellite measurements for an efficient interface to data assimilation. *Mon. Wea. Rev.*, **136**, 2633–2650.

Miyoshi, T., and M. Kunii, 2012: Using AIRS retrievals in the WRF-LETKF system to improve regional numerical weather prediction. *Tellus A*, **64**, 18408.

Morcrette, J. J., H. W. Barker, J. N. S. Cole, M. J. Iacono, and R. Pincus, 2008: Impact of a new radiation package, McRad, in the ECMWF integrated forecasting system. *Mon. Wea. Rev.*, **136**, 4773–4798.

O'Neill, L. L., D. B. Chelton, S. K. Esbensen, and F. F. Wentz, 2005: High-resolution satellite measurements of the atmospheric boundary layer response to SST variations along the Agulhas return current. *J. Climate*, **18**, 2706–2723.

Parkinson, C. L., 2003: Aqua: An Earth-observing satellite mission to examine water and other climate variables. *IEEE Trans. Geosci. Remote Sens.*, **41**, 265–273.

Parrish, D. F., and J. C. Derber, 1992: The national meteorological center's spectral statistical-interpolation analysis system. *Mon. Wea. Rev.*, **120**, 1747–1763.

Pu, Z., X. Li, and E. J. Zipser, 2009: Diagnosis of the initial and forecast errors in the numerical simulation of the rapid intensification of Hurricane Emily (2005). *Wea. Forecasting*, **24**, 1236–1251.

Pu, Z. X., and L. Zhang, 2010: Validation of atmospheric infrared sounder temperature and moisture profiles over tropical oceans and their impact on numerical simulations of tropical cyclones. *J. Geophys. Res.*, **115**, D24114, doi: 10.1029/2010JD014258.

Reale, O., J. Susskind, R. Rosenberg, E. Brin, E. Liu, L. P. Riishojgaard, J. Terry, and J. C. Jusem, 2008: Improving forecast skill by assimilation of quality-controlled AIRS temperature retrievals under partially cloudy conditions. *Geophys. Res. Lett.*, **35**, L08809, doi: 10.1029/2007GL033002.

Reale, O., W. K. Lau, J. Susskind, E. Brin, E. Liu, L. P. Riishojgaard, M. Fuentes, and R. Rosenberg, 2009: AIRS impact on the analysis and forecast track of tropical cyclone Nargis in a global data assimilation and forecasting system. *Geophys. Res. Lett.*, **36**, L06812, doi: 10.1029/2008GL037122.

Roy, C., and R. Kovordányi, 2012: Tropical cyclone track forecasting techniques—A review. *Atmospheric Research*, **104–105**, 40–69.

Skamarock, W.C., and Coauthors, 2008: A description of the Advanced Research WRF Version 3. NCAR Tech Note, NCAR/TN-475+STR, 113 pp. [Available online at http://www.mmm.ucar.edu/wrf/users/docs/arw_v3.pdf.]

Simpson, J., R. F. Adler, and G. R. North, 1988: A proposed tropical rainfall measuring mission (TRMM) satellite. *Bull. Amer. Meteor. Soc.*, **69**, 278–295.

Smith, W. L., E. Weisz, S. Kirev, D. Zhou, Z. Li, and E. Borbas, 2012: Dual-regression retrieval algorithm for real-time processing of satellite ultraspectral radiances. *J. Appl. Meteor. Climatol.*, **51**, 1455–1476.

Strow, L. L., S. E. Hannon, S. De-Souza Machado, H. E. Motteler, and D. Tobin, 2003: An overview of the AIRS Radiative Transfer Model. *IEEE Trans. Geosci. Remote Sens.*, **41**, 303–313.

Strow, L. L., S. E. Hannon, S. De-Souza Machado, H. E. Motteler, and D. C. Tobin, 2006: Validation of the atmospheric infrared sounder radiative transfer algorithm. *J. Geophys. Res.*, **111**, D09S06, doi: 10.1029/2005JD006146.

Susskind, J., 2007: Improved atmospheric soundings and error estimates from analysis of AIRS/AMSU data. *Proc. SPIE. 6684*, Atmospheric and Environmental Remote Sensing Data Processing and Utilization III: Readiness for GEOSS, 66840M (September 13, 2007), doi: 10.1117/12.734336.

Susskind, J., C. Barnet, and J. Blaisdell, 2003: Retrieval of atmospheric and surface parameters from AIRS/AMSU/HSB data in the presence of clouds. *IEEE Trans. Geosci. Remote Sens.*, **41**, 390–409.

Susskind, J., C. Barnet, J. Blaisdell, L. Iredell, F. Keita, L. Kouvaris, G. Molnar, and M. Chahine, 2006: Accuracy of geophysical parameters derived from Atmospheric Infrared Sounder/Advanced Microwave Sounding Unit as a function of fractional cloud cover. *J. Geophys. Res.*, **111**, D09S17, doi: 10.1029/2005JD006272.

Susskind, J., J. M. Blaisdell, L. Irdell, and F. Keita, 2011: Improved temperature sounding and quality control methodology using AIRS/AMSU Data: The AIRS Science Team Version 5 retrieval algorithm. *IEEE Trans. Geosci. Remote Sens.*, **49**, 883–907, doi: 10.1109/TGRS.2010.2070508.

Susskind, J., J. Blaisdell, and L. Iredell, 2012: Significant advances in the AIRS Science Team Version-6 retrieval algorithm. *Proc. SPIE* 8510, Earth Observing Systems XVII, 85100U (October 15, 2012), doi:10.1117/12.929953.

Tobin, D. C., and Coauthors, 2006: Atmospheric radiation measurement site atmospheric state best estimates for Atmospheric Infrared Sounder temperature and water vapor retrieval validation. *J. Geophys. Res.*, **111**, D09S14, doi: 10.1029/2005JD006103.

Weisz, E., J. Li, J. Li, D. K. Zhou, H.-L. Huang, M. D. Goldberg, and P. Yang, 2007: Cloudy sounding and cloud-top height retrieval from AIRS alone single field-of-view radiance measurements. *Geophys. Res. Lett.*, **34**, L12802, doi: 10.1029/2007GL030219.

Weisz, E., W. L. Smith Sr., and N. Smith, 2013: Advances in simultaneous atmospheric profile and cloud parameter regression based retrieval from high-spectral resolution radiance measurements. *J. Geophys. Res.*, **118**, 6433–6443.

Wentz, F., and T. Meissner, 2004: updated daily: AMSR-E/Aqua L2B Global Swath Ocean Products Derived from Wentz Algorithm V002, September 2008. National Snow and Ice Data Center. Boulder, Colorado USA. [Available online at http://nsidc.org/data/ae_ocean.html.]

Wentz, F. J., and T. Meissner, 2007: Supplement 1 Algorithm Theoretical Basis Document for AMSR-E Ocean Algorithms. RSS Tech. Report 051707, Remote Sensing Systems, Santa Rosa, California USA, 6 pp.

Won, Y.-I., 2008: Readme Document for AIRS Level-2 Version 5 Support Products. Goddard Earth Sciences Data and Information Services Center, National Aeronautics and Space Administration. 57 pp. [Available online at: http://disc.sci.gsfc.nasa.gov/AIRS/documentation/readmes/README.AIR-2SUP.pdf.]

Wu, L., and Coauthors, 2012: Relationship of environmental relative humidity with North Atlantic tropical cyclone intensity and intensification rate. *Geophys. Res. Lett.*, **39**, L20809, doi: 10.1029/2012GL053546.

Zavodsky, B. T., S. H. Chou, G. Jedlovec, and W. Lapenta, 2007: The impact of atmospheric infrared sounder (AIRS) profiles on short-term weather forecasts. *Proc. SPIE 6565*, Algorithms and Technologies for Multispectral, Hyperspectral, and Ultraspectral Imagery XIII, 65651J (May 07, 2007), doi:10.1117/12.718121.

Zhang, X., Q. Xiao, and P. Fitzpatrick, 2007: The impact of multisatellite data on the initialization and simulation of Hurricane Lili's (2002) rapid weakening phase. *Mon. Wea. Rev.*, **135**, 526–548.

Zhou, D. K.,W. L. Smith, X. Liu, A. M. Larar, S. A. Mango, and H.-L. Huang, 2007: Physically retrieving cloud and thermodynamic parameters from ultraspectral IR measurements. *J. Atmos. Sci.*, **64**, 969–982.